Iterative Trajectory Learning for Highly Accurate Optical Satellite Tracking Systems

Thomas Riel[a,*], Andreas Sinn[a], Christian Schwaer[a], Martin Ploner[b], Georg Schitter[a]

[a] *Automation and Control Institute (ACIN), TU Wien, Gußhausstraße 27-29, 1040, Vienna, Austria*
[b] *ASA Astrosysteme GmbH (ASA), Galgenau 19, 4212, Neumarkt i.M., Austria*

Abstract

This paper investigates the tracking accuracy of an optical telescope system used for satellite tracking and laser ranging applications. The investigated system uses a high precision motion controller and a pointing model based on spherical harmonics to achieve high accuracy. To overcome the limitations due to local pointing model inaccuracies and dynamic effects during tracking, an iterative trajectory learning algorithm is proposed. The implementation, as well as the stability analysis of the proposed concept is presented. Satellite tracking experiments are conducted to verify the accuracy of the proposed system. Utilizing the proposed iterative trajectory learning concept, the tracking error is reduced by a factor of 11 and is ultimately limited by the uncertainty of the orbit prediction.

Keywords: Iterative Learning Control, Precision Motion Control, Satellite Tracking, Satellite Laser Ranging, Space Debris Observation, Space Situation Awareness

1. Introduction

High performance optical satellite tracking is required for a range of applications, such as optical satellite communication (Hemmati et al. (2011); Kaushal and Kaddoum (2017)) and satellite laser ranging (Park et al. (2012)). These applications typically require a tracking precision in the sub-arcsecond range (Hemmati et al. (2011); Park et al. (2012); Kaushal and Kaddoum (2017)). Maintaining this level of precision over the entire operational envelope is a challenging task and requires detailed mechatronic analysis and controller design (Schmidt et al. (2014)).

However, the high precision of the tracking system is insufficient, if only low accuracy is achieved. This is particularly a challenge in mobile or cost efficient

*Corresponding author
Email address: riel@acin.tuwien.ac.at (Thomas Riel)

Pre-Print version of the article: Thomas Riel, Andreas Sinn, Christian Schwaer, Martin Ploner, Georg Schitter, "Iterative Trajectory Learning for Highly Accurate Optical Satellite Tracking Systems", *Acta Astronautica*, vol. 164, pp. 121-129, 2019. DOI: 10.1016/j.actaastro.2019.07.012

tracking systems, as high accuracy generally requires a very stable system and extensive calibration (Riel et al. (2019)).

The accuracy of satellite tracking systems is degraded by several factors, especially changing environmental conditions and sensor inaccuracies. Controlled environmental conditions, search algorithms, active tracking, and extensive calibration are usually employed to tackle these issues (Kaushal and Kaddoum (2017)). Changing environmental conditions in general and thermal deformations in particular are a main factor of pointing inaccuracy in the operation of optical telescope systems (Bely (2003); Gawronski (2007); Mittag et al. (2008)). Enclosures and thermal control systems are employed for larger telescopes to ensure suitable environmental conditions (Bely (2003); Bettonvil et al. (2008)). Special attention is also put on the telescope support structure to minimize residual movements (Hammerschlag et al. (2006)). Nevertheless, even the best designs experience remaining inaccuracies that lead to pointing errors.

Calibration is used to correct the repeatable pointing inaccuracies of a tracking system (Wallace (2002); Mittag et al. (2008)). The used pointing models are either based on a physical description of the telescope or purely empirical (Mittag et al. (2008)). To parametrize the pointing model, a number of observations at different positions are necessary. Using plate solving algorithms, the true position of the observations is determined and the error to the targeted position is calculated (Wallace (2002)). By also taking into account environmental factors, such as temperature, humidity or pressure, a fairly accurate pointing model can be constructed, with residual errors in the arcsecond range (Mittag et al. (2008); Schmitt et al. (2014)). However, this calibration can take a considerable fraction of a night (Schmitt et al. (2014)) and every change in the system makes a recalibration of the pointing model necessary. This is especially cumbersome for mobile telescope systems.

To reduce the required accuracy of the pointing model for optical satellite communication or laser ranging applications, search algorithms are used. Search algorithms together with optical feedback are usually employed within the acquisition phase (Kaushal et al. (2017)). The telescope searches the uncertainty region around the expected position following a certain search pattern. Optical feedback, e.g. from a beacon laser or an laser echo, is used to detect the true satellite position and its offset to the calculated position. Once the satellite is acquired, either the calculated trajectory with additional offset is followed in an open loop fashion, or active tracking is used.

Active tracking utilizes feedback from the satellite to adjust the telescope trajectory (Kaushal et al. (2017)). In optical communication, additional beacon beams are often used to align the optical ground station (OGS) with the space terminal, e.g. using a tracking sensor, such as a focal pixel array (FPA) or a 4-quadrant detector (4QD). Problems may arise when the tracking sensor is disturbed, e.g. by a bright star or cloud blockage. In such a case the satellite has to be re-acquired, which consumes valuable time during a satellite pass. The

Pre-Print version of the article: Thomas Riel, Andreas Sinn, Christian Schwaer, Martin Ploner, Georg Schitter, "Iterative Trajectory Learning for Highly Accurate Optical Satellite Tracking Systems", *Acta Astronautica*, vol. 164, pp. 121-129, 2019. DOI: 10.1016/j.actaastro.2019.07.012

tracking sensor also diverts light from the receiver and is usually too complex for cost efficient telescope systems.

None of the above solutions is well suited for the targeted segment of cost efficient or mobile satellite tracking systems. To solve this issue a new approach is investigated.

In other precision engineering tasks, iterative learning control (ILC) is often applied to achieve highly accurate results for repeating motions (Bristow et al. (2006); Yoo et al. (2016)). ILC utilizes the stored input and achieved error of the previous iteration to reshape the input signal of the current iteration. Using ILC improvements of two orders of magnitude have been achieved, e.g. in scanning microscopy applications (Yoo et al. (2016)).

The contribution of this paper is the application of the ILC concept to improve the tracking performance of mobile or cost efficient telescope systems. For this purpose, the desired satellite trajectory is calculated and trained shortly before the actual satellite pass. The star background together with a plate solving algorithm is used as absolute position sensor during the training phase. This trajectory learning phase with sensor feedback allows for the elimination of static, as well as dynamic errors within the telescope system. The optimized satellite trajectory is then followed in an open loop fashion during the actual satellite pass, allowing all light to be used for the observation or the scientific instrument. Tracking experiments using low earth orbit (LEO) as well as medium earth orbit (MEO) satellites are conducted to confirm the improved tracking accuracy of the proposed system.

The remaining paper is organized as follows. Section 2 provides a description of the system used in this investigation. The proposed concept and ILC design is presented in Section 3. The implementation of the star sensor is described in Section 4, followed by a description of the used satellite targets in Section 5. Section 6 presents the conducted tracking experiments and their results. Finally, the conclusion and outlook is provided in Section 7.

2. System description

2.1. Tracking system

The investigated system consists of a DDM60 mount and a N300/1140 telescope (both: ASA Astrosysteme GmbH, Neumarkt i. M., Austria), is shown in Figure 1. Two direct-drive permanent magnet synchronous motors (PMSMs) are used to actuate the two axes, which are aligned to the altitude (alt) and azimuth (az) axes. A short overview of the motor parameters is given in Table 1. The position of the tracking system is measured by optical absolute encoders with a noise floor of 160 nrad root mean square (RMS) and a sampling rate of 20 kHz.

Pre-Print version of the article: Thomas Riel, Andreas Sinn, Christian Schwaer, Martin Ploner, Georg Schitter, "Iterative Trajectory Learning for Highly Accurate Optical Satellite Tracking Systems", *Acta Astronautica*, vol. 164, pp. 121-129, 2019. DOI: 10.1016/j.actaastro.2019.07.012

Figure 1: Investigated satellite tracking system developed together with ASA Astrosysteme GmbH, mounted on a test site in Upper Austria. Also visible on top of the tube is the optical breadboard with tertiary mirror and camera.

Table 1: Motor parameters of the telescope system.

	alt-axis	az-axis
Rated current I_{nom}	3.4 A	5.8 A
Number of pole pairs Z_p	11	11
Resistance R	1.31 Ω	0.98 Ω
Inductance L_q	3.3 mH	5.4 mH
Torque constant k_m	1.84 N m/A	2.43 N m/A

The system can be attached to a solid support as well as a tripod and is easily transportable.

A GPS timing module (NEO-M8T, u-blox AG, Thalwil, Switzerland) is directly connected to the motion controller of the telescope mount, in order to provide a precise time reference with an accuracy in the sub-µs range. This time reference is also used to constantly calibrate the internal quartz oscillator, thereby allowing to bridge a potential temporary loss of the GPS signal.

The system is intended as cost effective, semi-mobile ground station for optical satellite communication, satellite laser ranging (SLR), space debris observation, as well as general scientific investigations. For these purposes, the system should be able to track LEO, as well as MEO satellites with a velocity of up to one degree per second (dps), with a tracking precision in the sub-arcsecond range.

Pre-Print version of the article: Thomas Riel, Andreas Sinn, Christian Schwaer, Martin Ploner, Georg Schitter, "Iterative Trajectory Learning for Highly Accurate Optical Satellite Tracking Systems", *Acta Astronautica*, vol. 164, pp. 121-129, 2019. DOI: 10.1016/j.actaastro.2019.07.012

Table 2: Optical parameters of the telescope and camera system.

Aperture diameter d	30 cm
Focal length f	1140 mm
Configuration	Newtonian
Sensor size w x h	2560 x 2160 px
Field of view FOV	0.84 x 0.71 °
Max. quantum efficiency QE	60 %
Pixel size p	6.5 μm
Read noise S_r	1.2 e^-
Dark current I_d	0.1 e^-/s/px
Spectral bandwidth B	300 − 1000 nm
Fill factor FF	90 %
Max. frame rate fr	100 Hz

The cost of the system is intended to be close to the goal set by the Massachusetts Institute of Technology portable telescope for lasercom (MIT-PorTeL) (Riesing et al. (2017)), which lies more than one order of magnitude below current high performance tracking systems. Dynamic error budgeting is employed to optimize the mechatronic system (Riel et al. (2017)) and a robust disturbance-observer based control system is implemented to achieve high precision tracking (Riel et al. (2018)). Previous work has demonstrated tracking of LEO, as well as MEO satellites with velocities of up to one dps and seeing limited precision, i.e. with internal encoder errors below the arcsecond range (Riel et al. (2019)). However, the absolute accuracy for satellite targets is still insufficient.

2.2. Optical system

A Newtonian telescope with 30 cm aperture size, together with a flat tertiary mirror and a 5.5 Megapixel sCMOS camera (Zyla 5.5, Andor Technology Ltd, Belfast, Northern Ireland) form the optical system. The sCMOS camera is cooled by a peltier element to an operating temperature of 0 °C. An overview of the most important parameters of the optical system is given in Table 2.

Preliminary experiments (data not shown) have verified, that using this setup with 20 ms exposure time, objects with an apparent visual magnitude m_v of 12 are reliably detectable using algorithmic means. This means, that within the field of view (FOV) of the system, approximately 34 detectable stars can be expected (Berry and Burnell (2000)). This number of stars is sufficient for plate solving algorithms and therefore for the proposed iterative trajectory learning algorithm.

Pre-Print version of the article: Thomas Riel, Andreas Sinn, Christian Schwaer, Martin Ploner, Georg Schitter, "Iterative Trajectory Learning for Highly Accurate Optical Satellite Tracking Systems", *Acta Astronautica*, vol. 164, pp. 121-129, 2019. DOI: 10.1016/j.actaastro.2019.07.012

3. Iterative trajectory learning

3.1. Trajectory learning concept

The proposed iterative trajectory learning approach is based on iterative learning control (ILC) (Bristow et al. (2006)). ILC is widely used in iterative motion control applications to improve the accuracy of repetitive motion trajectories. Applying the ILC concept to satellite tracking applications may therefore yield in comparable improvements in accuracy. However, satellite tracking applications per se are not iterative tasks as every pass is different from one another. But the satellite trajectory can still be learned by using the pre-calculated trajectory together with an absolute position sensor. By learning the satellite trajectory based on the star background shortly before the actual satellite pass, all consistent and repeatable, static as well as dynamic errors can be eliminated, thereby improving the accuracy of the tracking system. A plate solving algorithm, as described in 4, is used to solve the star background of every training pass, thereby forming an absolute position sensor. Figure 2 illustrates the proposed iterative trajectory learning concept, which consists of two parts:

1. Training phase, where the pre-calculated satellite trajectory is optimized during N-1 iterations prior to the satellite pass, using the star background as reference.
2. Satellite pass, where the satellite is tracked without any feedback and all light can be used for the observation or the scientific instrument.

During the first iteration, shown in Figure 2 (a), the pre-calculated satellite trajectory r_1 (black, solid) is used to form the input u_1 (blue, dashed) of the motion control system. The camera system is used to observe the sky background during the trajectory. These observations are then solved for their coordinates, allowing the reconstruction of the achieved trajectory y_1 (red, dotted). Based on this measurement of the actual trajectory y_1, an error e_1 is calculated. This error e_1 is then used to correct the initial trajectory r_1 to form the new trajectory $r_2(e_1, r_1)$. This new trajectory r_2 is then used in the second iteration Figure 2 (b) to form the input u_2 for the motion control system. Using this improved trajectory u_2, a more accurate result y_2 is obtained. This learning process can be repeated N times before the final iteration (Figure 2 (c)), which is the actual satellite pass. As no camera based tracking is required during the satellite pass (blind tracking), all light can be used for the observation or the scientific instrument.

The following list sums up the individual steps of the proposed iterative trajectory learning:

1. Pre-calculate satellite trajectory r_1 based on satellite orbit.
2. Use r_1 to form input u_1 for motion control system.
3. Observe and solve sky background to reconstruct achieved trajectory y_1.

Pre-Print version of the article: Thomas Riel, Andreas Sinn, Christian Schwaer, Martin Ploner, Georg Schitter, "Iterative Trajectory Learning for Highly Accurate Optical Satellite Tracking Systems", *Acta Astronautica*, vol. 164, pp. 121-129, 2019. DOI: 10.1016/j.actaastro.2019.07.012

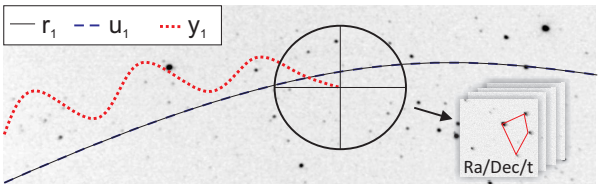

(a) Iteration 1, $t = -\tau_1$

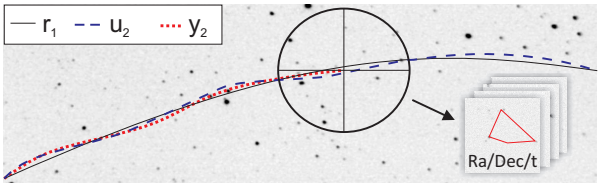

(b) Iteration 2, $t = -\tau_2$

$\vdots$

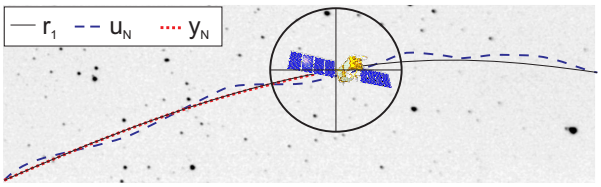

(c) Iteration N, $t = 0$

Figure 2: Illustration of the proposed iterative trajectory learning concept. In the first iteration (a) the pre-calculated satellite trajectory r_1 (black, solid) is used to form the input u_1 for the motion control system (blue, dashed). During the trajectory, the camera system observes the sky background. These observations are then solved for their coordinates, allowing the reconstruction of the achieved trajectory y_1 (red, dotted). Based on this measurement, a trajectory error e_1 is calculated, which is used to correct the initial trajectory r_1. This corrected trajectory r_2 is then used to form the input u_2 for the next iteration (b), thereby achieving an improved accuracy. This iterative learning process can be repeated N times before the final iteration (c), which is also the satellite pass. During the final pass, all light can be used for the observation or the scientific instrument, as the trajectory is performed without optical feedback.

Pre-Print version of the article: Thomas Riel, Andreas Sinn, Christian Schwaer, Martin Ploner, Georg Schitter, "Iterative Trajectory Learning for Highly Accurate Optical Satellite Tracking Systems", *Acta Astronautica*, vol. 164, pp. 121-129, 2019. DOI: 10.1016/j.actaastro.2019.07.012

4. Form error e_1 between desired trajectory r_1 and achieved trajectory y_1.
5. Derive an improved trajectory r_2 by correcting r_1 using the error e_1.
6. Iterate to step 2 using the corrected trajectory.
7. For the actual satellite pass use the trajectory r_N to form input u_N for the motion control system. As no camera is required, all light can be used for the observation or the scientific instrument.

3.2. Iterative learning control

The correction of the trajectory y based on the error e is achieved using an ILC algorithm. A plant inversion based ILC algorithm is chosen in this investigation (de Roover (1996); Bristow et al. (2006)). Using a description in the z-domain, the used ILC learning algorithm can be described by

$$U_{\mathrm{j}+1}(z) = Q(z)\,[U_{\mathrm{j}}(z) + \rho\,L(z)\,E_{\mathrm{j}}(z)], \tag{1}$$

where $U_{\mathrm{j}}(z)$ is the z-transform of the input of the j^{th} iteration, $Q(z)$ and $L(z)$ are filters, ρ is the learning gain and $E_{\mathrm{j}}(z)$ is the z-transform of the error of the j^{th} iteration. By varying the learning gain ρ between zero and one, the learning rate can be influenced. For this description, ρ is assumed to be one, i.e. fastest learning rate.

The learning filter L and the filter Q are the available design variables. For plant inversion based ILC algorithms, the filter Q is usually a low-pass filter, often described as robustness filter for the learning performance (de Roover (1996)). L on the other hand corresponds to the inverse of the controlled plant P. In order to guarantee asymptotic stability, the condition (de Roover (1996))

$$\|Q(z)\,[1 - L(z)\,P(z)]\|_\infty < 1, \tag{2}$$

has to be fulfilled, where $P(z)$ is the plant and $\|\cdot\|_\infty$ represents the H_∞-norm.

To achieve a fast learning rate, the bandwidth of Q should be as high as possible, given the plant uncertainty and therefore uncertainty of L. For the proposed iterative trajectory learning, the plant P is given by the complementary sensitivity function T, i.e. the closed loop behavior of the telescope motion control system.

3.3. ILC implementation

As briefly described in Section 2, the used sensor system utilized a sCMOS camera together with a plate solving algorithm to measure the actual position of the tracking system. To achieve an accurate timing, the camera is integrated with the high level motion control software of the telescope mount. This implementation allows a maximum acquisition rate of 30 frames per second. Hence, the sampling rate of the ILC is set to 30 Hz and therefore also the bandwidth of both filters is limited to half of this sampling rate.

Pre-Print version of the article: Thomas Riel, Andreas Sinn, Christian Schwaer, Martin Ploner, Georg Schitter, "Iterative Trajectory Learning for Highly Accurate Optical Satellite Tracking Systems", *Acta Astronautica*, vol. 164, pp. 121-129, 2019. DOI: 10.1016/j.actaastro.2019.07.012

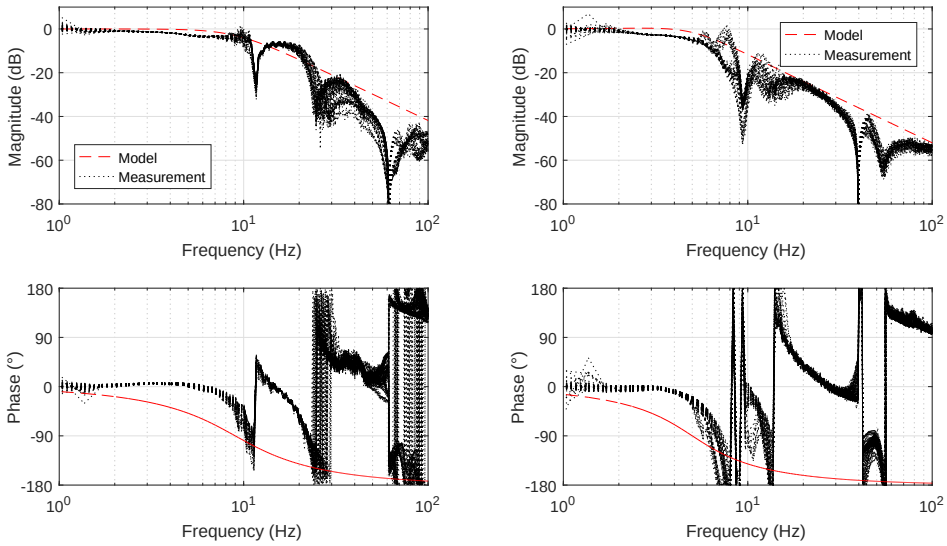

Figure 3: Bode diagram of the complementary sensitivity function T at various telescope poses (black, dotted) and the used second order model (red, dashed) (a) for the alt-axis and (b) for the az-axis.

To investigate the stability of the ILC, $L = T^{-1}$ is assumed. The complementary sensitivity function T of the telescope is recorded at various telescope poses, spanning the full operational envelope. This allows the investigation of the plant uncertainty and stability over the full working range. The mean closed loop behavior of the system can be described by a second order low-pass with butterworth characteristic and a bandwidth of 9 Hz for the alt-axis and 5 Hz for the az-axis (Riel et al. (2019)). The bode diagram of the set of complementary sensitivity functions of the alt-axis and the az-axis is shown in Figure 3 (a) and Figure 3 (b), respectively. Dominant dynamics (anti-resonance at 9 Hz to 11 Hz) limit the achievable motion control bandwidth.

A second order butterworth low-pass filter is used as Q-filter. The bandwidth is adjusted such that the stability condition (2) if fulfilled. A graphic representation of this condition is shown in Figure 4 (a) for the alt-axis and (b) for the az-axis. Stability is guaranteed as long as $Q(z)\,[1-L(z)\,P(z)]$ (black, dotted) stays within the unit circle (red, solid). This is the case for a Q-filter bandwidth of 11 Hz and 7 Hz for the alt-axis and az-axis, respectively.

Pre-Print version of the article: Thomas Riel, Andreas Sinn, Christian Schwaer, Martin Ploner, Georg Schitter, "Iterative Trajectory Learning for Highly Accurate Optical Satellite Tracking Systems", *Acta Astronautica*, vol. 164, pp. 121-129, 2019. DOI: 10.1016/j.actaastro.2019.07.012

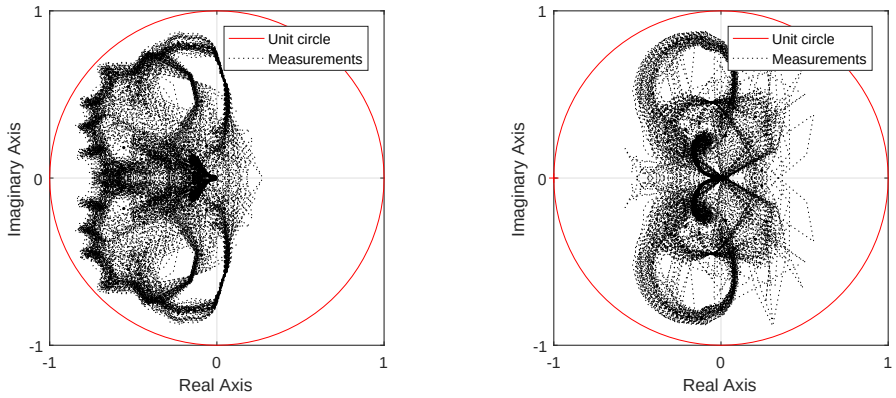

Figure 4: Graphical representation of the stability condition (2) (a) for the alt-axis and (b) for the az-axis. Stability is given as long as $Q(z)\,[1 - L(z)\,P(z)]$ (black, dotted) remains within the unit circle (red, solid) at all possible telescope poses.

4. Plate solving and pointing model

4.1. Plate solving algorithm

To retrieve the pointing information of the images observed during the learning phase, the *Astrometry.net* framework is used (Lang et al. (2010)). *Astrometry.net* is a robust astrometry system, which is based on geometric hashing using star quads. Using this framework, the celestial coordinates of the observed camera images in the FITS World Coordinate System (WCS) (Calabretta and Greisen (2002)) are computed. This positional information is then transformed into topocentric coordinates, which are used for the satellite trajectory. Utilizing local weather data, corrections for astronomical and satellite refraction are considered in this transformation (Seeber (2008)).

The implementation of the plate solving algorithm is based on a stand-alone instance of *Astrometry.net* together with an appropriate interface integrated into the high level motion control software of the telescope mount. To speed up the plate solving, up to twelve parallel *Astrometry.net* processes are used. With an average solving time of two seconds per image, up to six images per second can be solved. This allows a one minute pass to be solved in approx. two and a half minutes, which means that three iterations can be performed in eleven minutes prior to the satellite pass. While this paper focused on the feasibility, using better paralleling and improved computation power will allow significant reduction of the solving time in the future.

The precision of the plate solving algorithm is ultimately limited by the atmospheric seeing conditions. Static experiments with 20 ms exposure time show a standard deviation of 0.6″ and 1.1″ in the alt and az-axis, respectively. This is

Pre-Print version of the article: Thomas Riel, Andreas Sinn, Christian Schwaer, Martin Ploner, Georg Schitter, "Iterative Trajectory Learning for Highly Accurate Optical Satellite Tracking Systems", *Acta Astronautica*, vol. 164, pp. 121-129, 2019. DOI: 10.1016/j.actaastro.2019.07.012

well within the atmospheric seeing conditions at the experiment location (Mauthausen, Austria) and also reflects the predominant wind direction present during the experiment.

4.2. Pointing model

The plate solving algorithm is also the basis for the used pointing model. To correct static pointing errors of the system, a calibration based on a set of spherical harmonics $Y_l^m(\theta, \varphi)$ is used. Here $Y_l^m(\theta, \varphi)$ represents the spherical harmonic of degree l and order m with the alt-angle θ and the az-angle φ.

The spherical harmonics of up to degree and order three are supplemented by an additional plane in Cartesian coordinates to form the set of base functions for the calibration. This results in 26 parameters that are determined based on 40 to 60 pointing measurements over the entire working range, using least squares parameter estimation. For the used setup, this parameter estimation results in a residual RMS fitting error of $9''$ over the investigated working range. This is still a considerable error when compared to the accuracy requirements and represents only the quality of the achieved model fit and not the accuracy of the model itself. However, compared to a simple plane calibration, using this pointing model an improvement by two orders of magnitude is achieved.

5. Tracking targets and orbit prediction

5.1. Tracking targets

To evaluate the proposed iterative trajectory learning, a number of satellite targets is selected. The satellites include LEO as well as MEO satellites with a wide variety of orbits. To allow a simple optical verification, only visible passes are chosen, i.e. when the satellite is illuminated by the sun in a way that makes it visible from the ground station. A list of the selected objects is provided in Table 3. The visible brightness varies considerably between the individual satellites, but remains within the observable limits of the camera system.

5.2. Orbit prediction

The orbit of the satellites is predicted using consolidated prediction format (CPF) data of the international laser ranging service (ILRS) (Pearlman et al. (2002)) sourced from *cddis.nasa.gov* (Noll (2018)), or two-line element sets (TLEs), which are sourced from *celestrak.com* (Kelso (2018)). The two different orbit sources are expected to show different absolute accuracy, with the CPF data being the most accurate. Experiments show, that the expected prediction accuracy of up to date TLEs lies in the tens of arcsecond range, while the accuracy for CPFs lies in the arcsecond range. An exemplary comparison between the orbit prediction accuracy for the satellite AJISAI (NORAD ID: 16908) using TLEs and CPFs is shown in Figure 5.

Pre-Print version of the article: Thomas Riel, Andreas Sinn, Christian Schwaer, Martin Ploner, Georg Schitter, "Iterative Trajectory Learning for Highly Accurate Optical Satellite Tracking Systems", *Acta Astronautica*, vol. 164, pp. 121-129, 2019. DOI: 10.1016/j.actaastro.2019.07.012

Table 3: List of targets used for the performed tracking experiments.

Name	NORAD ID	Perigee	Apogee	Orbit Source
BREEZ-M DEB	36501	331 km	13 138 km	TLE
ISS	25544	409 km	415 km	TLE
CRYOSAT-2	36508	719 km	732 km	CPF
ENVISAT	27386	772 km	773 km	CPF
ATLAS 2AS CENTAUR R/B	26906	805 km	1398 km	TLE
H-2 R/B	24279	865 km	1314 km	TLE
THORAD AGENA D R/B	05679	937 km	953 km	TLE
USA 194 DEB	31708	941 km	1287 km	TLE
COSMOS-2344	24827	1278 km	2979 km	TLE
JASON-2	33105	1312 km	1324 km	CPF
JASON-3	41240	1339 km	1350 km	CPF
AJISAI	16908	1486 km	1504 km	CPF
LAGEOS-2	22195	5622 km	5959 km	CPF
ETALON-1	19751	19 077 km	19 189 km	CPF
GLONASS-102	29670	19 082 km	19 192 km	CPF
GLONASS-103	29671	19 092 km	19 182 km	CPF
GLONASS-126	37829	19 119 km	19 155 km	CPF
BEIDOU-3M3	43208	21 516 km	21 554 km	CPF
GALILEO-205	40889	23 221 km	23 238 km	CPF

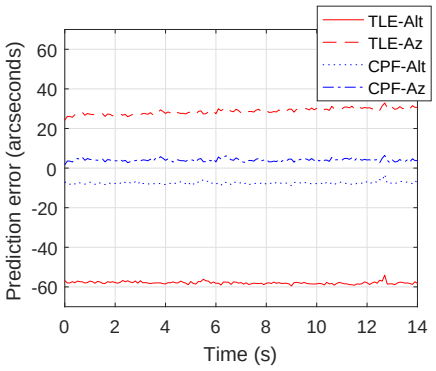

Figure 5: Comparison of the prediction error between TLEs and CPFs for the satellite AJISAI (NORAD ID: 16908), recorded on the 19th of September 2018, 21:39:36 UTC. The mean prediction error for TLEs is 43.2″, while for CPFs the mean error is 5.6″.

Pre-Print version of the article: Thomas Riel, Andreas Sinn, Christian Schwaer, Martin Ploner, Georg Schitter, "Iterative Trajectory Learning for Highly Accurate Optical Satellite Tracking Systems", *Acta Astronautica*, vol. 164, pp. 121-129, 2019. DOI: 10.1016/j.actaastro.2019.07.012

The initial orbit prediction is the starting point for the iterative trajectory learning, as described in Section 3. For TLEs, the orbit prediction is carried out using a SGP4 propagator (Rino (2010)). For CPFs, the C interpolator implementation provided by the ILRS is utilized (Gurtner and Ricklefs (2005)).

6. Tracking experiments

To evaluate the accuracy of the proposed trajectory learning, tracking experiments are carried out. Based on the initial orbit prediction, iterative trajectory learning, as described in Section 3, is conducted. Once the learning process is completed, the trajectory is carried out in an open-loop fashion without any visual feedback, i.e. blind tracking. However, the camera observations are used afterwards to evaluate the achieved accuracy.

In total, 43 verification experiments are carried out in Mauthausen (Austria) over a duration of 16 days in September of 2018. The individual experiments have durations between 15 and 90 seconds and are performed at various altitudes, ranging from 25° to 81°.

Figure 6 shows an exemplary tracklet with 25 seconds duration of a debris segment of the rocket body Breeze-M (NORAD ID: 36501). The tracklet was recorded on 23:43:18 UTC at the 18$^{\text{th}}$ of September 2018. It starts at an altitude of 73° and has a maximal angular velocity of one dps. Two obstructions due to clouds are visible in the first third of the tracklet. Also visible at the start of the tracklet is the initial acceleration phase of the tracking system.

Figure 7 depicts a stack of twenty individual exposures of the satellite JASON-2 (NORAD ID: 33105) taken on 20$^{\text{th}}$ of September 2018. A closer view is depicted in Figure 8, where a stacked image of 250 individual exposures of the satellite (a) ATLAS 2AS CENTAUR R/B (NORAD ID: 26906) and (b) JASON-3 (NORAD ID: 41240), observed on 20$^{\text{th}}$ of September 2018 at 23:15:59 UTC and 01:26:00 UTC, respectively. The red cross marks the image center, while passing stars are visible as dashed lines. No alignment procedure was applied in the stacking process. The satellite observations, taken with the camera, are used to evaluate the achieved tracking error.

The result of a tracking experiment without prior trajectory learning, is shown in Figure 9, for the satellite JASON-2 (NORAD ID: 33105) recorded on 26$^{\text{th}}$ of September 2018 at 23:13:42 UTC. Shown are the internal encoder errors e_{enc} of the telescope mount together with the observed, optical tracking error e_{opt} reconstructed from the camera observations. Based on the internal encoder error e_{enc}, it can be concluded that the motion control system performs an accurate and precise motion. However, the achieved optical tracking error of the satellite target e_{opt} is in the 80″ range.

Despite the use of an extensive pointing model, the error e_{opt} is one order of magnitude larger than desired. This mismatch may well be attributed to the

Pre-Print version of the article: Thomas Riel, Andreas Sinn, Christian Schwaer, Martin Ploner, Georg Schitter, "Iterative Trajectory Learning for Highly Accurate Optical Satellite Tracking Systems", *Acta Astronautica*, vol. 164, pp. 121-129, 2019. DOI: 10.1016/j.actaastro.2019.07.012

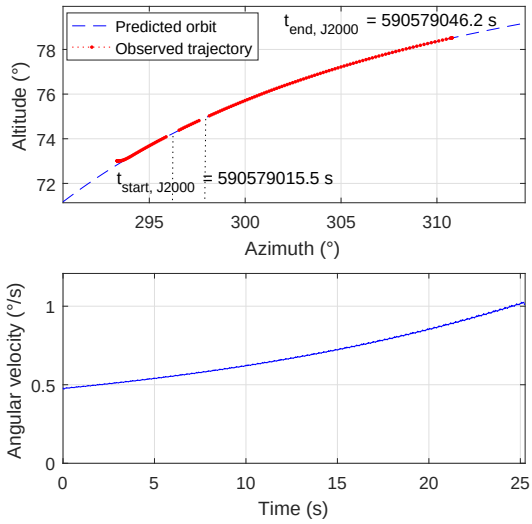

Figure 6: Tracklet with 25 seconds duration of debris of the rocket body Breeze-M (NORAD ID: 36501), recorded on the 18th of September 2018, 21:43:35 UTC, with a mean angular velocity of 0.71 dps. Also visible is the acceleration sequence at the start of the trajectory and two obstructions due to cloud cover in the first third of the tracklet (at an az-angle of 296° and 298°).

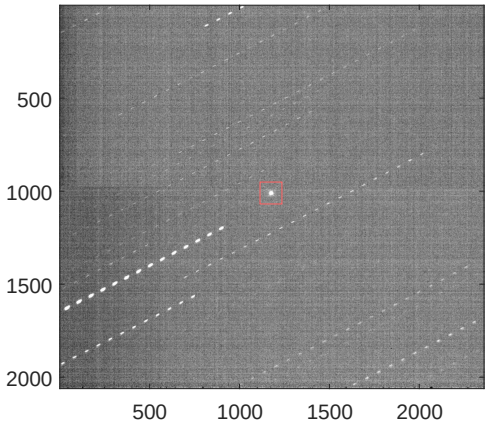

Figure 7: Stack of twenty images taken of the satellite JASON-3 (NORAD ID: 41240) on 20th of September 2018. The satellite is marked with a red square of 150″ size. Passing stars can be seen as dashed lines in the stacked image.

Pre-Print version of the article: Thomas Riel, Andreas Sinn, Christian Schwaer, Martin Ploner, Georg Schitter, "Iterative Trajectory Learning for Highly Accurate Optical Satellite Tracking Systems", *Acta Astronautica*, vol. 164, pp. 121-129, 2019. DOI: 10.1016/j.actaastro.2019.07.012

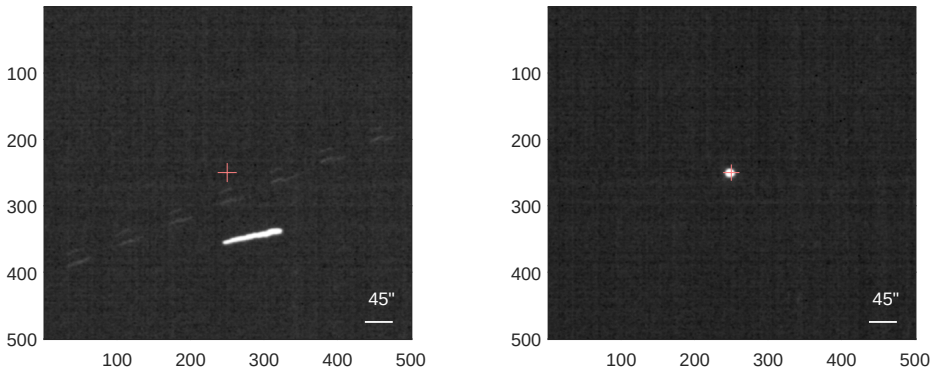

Figure 8: Stack of 250 images taken of the satellites (a) CENTAUR R/B (NORAD ID: 26906) without iterative trajectory learning and (b) JASON-3 (NORAD ID: 41240) with trajectory learning. The image center is marked with a red cross. Passing stars can be seen as dashed lines in the stacked image.

local uncertainty of the pointing model as well as unobservable dynamic effects during the tracking. To achieve a higher accuracy, iterative trajectory learning is used.

Figure 10 (a) shows the evolution of the tracking error for the satellite LAGEOS-2 (NORAD ID: 22195) over the course of six iterations. After two training runs, the error is reduced by a factor of 77 to 1.8″. At this level the error is well below the fitting accuracy of the pointing model and approaching the limit of the plate solving algorithm.

Figure 10 (b) shows the achieved tracking error during the final satellite pass on 17$^{\text{th}}$ of September 2018 at 22:22:18 UTC. The mean tracking error is 2.8″ with a standard deviation of 0.6″, resulting in an accuracy that is limited by the remaining uncertainty in the orbit prediction as well as the plate solving algorithm.

Figure 11 (a) shows the evolution of the tracking error for the satellite JASON-3 (NORAD ID: 41240) over the course of ten iterations. After three iterations, the error is reduced by a factor of 50 to 6″. After seven more iterations the error is reduced by another factor of two down to 3″. This indicates that most of the improvement is already achieved after only two training runs.

Figure 11 (b) shows the achieved tracking error during the final satellite pass, as well as the internal encoder error. The mean tracking error is reduced to 8″ with a standard deviation of 0.7″. The difference between the tracking error during training and the final tracking error can be explained by the uncertainty of the orbit prediction, which is in the arcsecond range (compare Figure 5).

Pre-Print version of the article: Thomas Riel, Andreas Sinn, Christian Schwaer, Martin Ploner, Georg Schitter, "Iterative Trajectory Learning for Highly Accurate Optical Satellite Tracking Systems", *Acta Astronautica*, vol. 164, pp. 121-129, 2019. DOI: 10.1016/j.actaastro.2019.07.012

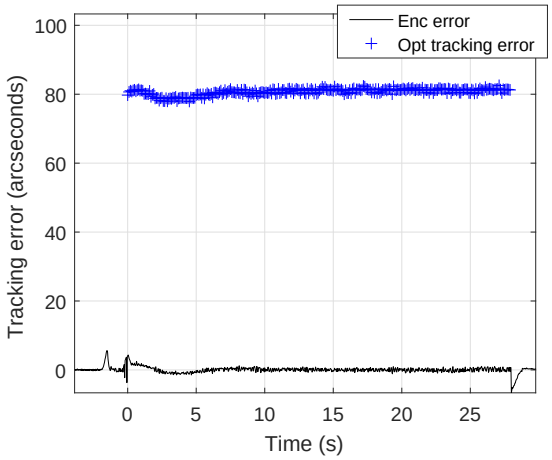

Figure 9: Tracking error of the satellite JASON-2 (NORAD ID: 33105) on 26$^{\text{th}}$ of September 2018 at 23:13:42 UTC. Shown is the internal encoder error (black, solid) together with the optical tracking error (blue cross). Although an extensive pointing model is used, the optical tracking error is one order of magnitude above the desired level.

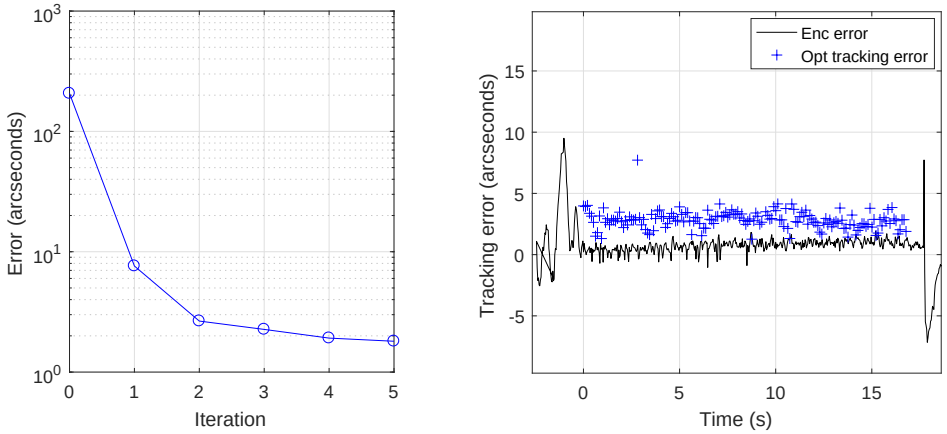

Figure 10: Tracking error of the satellite LAGEOS-2 (NORAD ID: 22195) on 17$^{\text{th}}$ of September 2018. (a) tracking error during the learning process as a function of the number of performed iterations and (b) internal encoder error (black, solid) and optical tracking error (blue cross) during the final pass at 22:22:18 UTC.

Pre-Print version of the article: Thomas Riel, Andreas Sinn, Christian Schwaer, Martin Ploner, Georg Schitter, "Iterative Trajectory Learning for Highly Accurate Optical Satellite Tracking Systems", *Acta Astronautica*, vol. 164, pp. 121-129, 2019. DOI: 10.1016/j.actaastro.2019.07.012

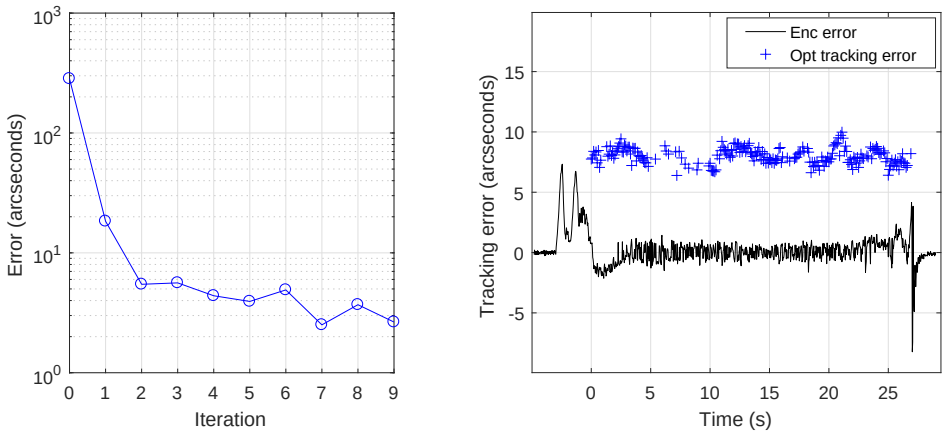

(a) (b)

Figure 11: Tracking error of the satellite JASON-3 (NORAD ID: 41240) on 20$^{\text{th}}$ of September 2018. (a) tracking error during the learning process as a function of the number of performed iterations and (b) internal encoder error (black, solid) and optical tracking error (blue cross) during the final pass at 01:26:00 UTC.

These experimental results, summarized in Figure 12, verify the function and capabilities of the proposed iterative trajectory learning algorithm. Figure 12 compares the achieved tracking error for the different satellite orbit prediction methods with and without iterative trajectory learning. For satellites with TLE data, a factor of 6 improvement is achieved, while for satellites with more precise CPF data, a factor of 11 improvement is achieved. During the learning phase, the accuracy appears to be limited by the plate solving algorithm. However, the final satellite pass also reveals the remaining uncertainty in the orbit prediction, which puts an ultimate limit on the achievable accuracy. For a one minute pass, approx. eleven minutes are sufficient to perform three training runs. With a fast learning rate, this low number of iterations is sufficient to significantly improve the tracking accuracy.

Using the proposed concept, the tracking error is improved by a factor of 6 for satellites with TLE data and by a factor of 11 for satellites with CPF data to a level that is well below the fitting accuracy of the used pointing model.

7. Conclusion

A novel iterative trajectory learning algorithm for highly accurate satellite tracking is proposed and its implementation discussed. The stability of the algorithm in presence of position dependent plant uncertainties is analyzed. The

Pre-Print version of the article: Thomas Riel, Andreas Sinn, Christian Schwaer, Martin Ploner, Georg Schitter, "Iterative Trajectory Learning for Highly Accurate Optical Satellite Tracking Systems", *Acta Astronautica*, vol. 164, pp. 121-129, 2019. DOI: 10.1016/j.actaastro.2019.07.012

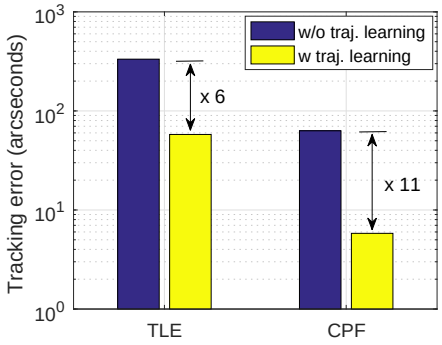

Figure 12: Comparison of the achieved tracking error for the different satellite orbit prediction methods, with (right, yellow) and without (left, blue) iterative trajectory learning.

implemented pointing model is described and its parametrization discussed. Experimental verification is carried out using blind tracking of various satellites. Compared to the satellite tracking using only the pointing model, the proposed iterative trajectory learning approach achieves a factor 6 improvement in accuracy for satellites with TLE data and a factor 11 improvement in accuracy for satellites with CPF data. This allows the system to operate with a tracking accuracy that is mainly limited by the uncertainty of the orbit prediction.

Utilizing the proposed algorithm, the investigated system can be used as a cost effective optical ground station for highly accurate and precise blind tracking of satellites. This enables a wide range of users to gain access to a range of applications, such as optical satellite communication or space debris observation.

Acknowlegements

The authors gratefully acknowledge the excellent cooperation with ASA Astrosysteme GmbH and thank for their support and valuable expertise.

This work was funded by the Austrian research funding association (FFG) under the scope of the Bridge program (contract number 850722).

References

H. Hemmati, A. Biswas, and I. B. Djordjevic. Deep-space optical communications: Future perspectives and applications. *Proceedings of the IEEE*, 99(11): 2020–2039, 2011.

H. Kaushal and G. Kaddoum. Optical communication in space: Challenges and mitigation techniques. *IEEE Communications Surveys Tutorials*, 19(1):57–96, 2017.

Pre-Print version of the article: Thomas Riel, Andreas Sinn, Christian Schwaer, Martin Ploner, Georg Schitter, "Iterative Trajectory Learning for Highly Accurate Optical Satellite Tracking Systems", *Acta Astronautica*, vol. 164, pp. 121-129, 2019. DOI: 10.1016/j.actaastro.2019.07.012

C. H. Park, Y. S. Son, B. I. Kim, S. Y. Ham, S. W. Lee, and H. C. Lim. Design of tracking mount and controller for mobile satellite laser ranging system. *Advances in Space Research*, 49(1):177–184, 2012.

R.M. Schmidt, G. Schitter, A. Rankers, and J. van Eijk. *The Design of High Performance Mechatronics*. IOS Press, Amsterdam, 2nd edition, 2014.

T. Riel, A. Galffy, G. Janisch, D. Wertjanz, A. Sinn, C. Schwaer, and G. Schitter. High performance motion control for optical satellite tracking systems. *Advances in Space Research, (submitted)*, 2019.

P. Y. Bely, editor. *The Design and Construction of Large Optical Telescopes*. Berlin, New York: Springer, 2003.

Wodek Gawronski. Control and pointing challenges of large antennas and telescopes. *IEEE Transactions on Control Systems Technology*, 15(2):276–289, 2007.

M. Mittag, A. Hempelmann, J. N. Gonzalez-Perez, and J. H. M. M. Schmitt. The temperature dependence of the pointing model of the hamburg robotic telescope. *Publications of the Astronomical Society of the Pacific*, 120(866): 425, 2008.

F. C. M. Bettonvil, R. H. Hammerschlag, A. P. L. Jägers, and G. Sliepen. Large fully retractable telescope enclosures still closable in strong wind. In *Advanced Optical and Mechanical Technologies in Telescopes and Instrumentation*, volume 7018, page 70181N. International Society for Optics and Photonics, 2008.

R. H. Hammerschlag, F. C. M. Bettonvil, and A. P. L. Jägers. Towers for telescopes with extreme stability: active or passive? In *Optomechanical Technologies for Astronomy*, volume 6273, page 62731O. International Society for Optics and Photonics, 2006.

P. T. Wallace. A rigorous algorithm for telescope pointing. In *Advanced Telescope and Instrumentation Control Software II*, volume 4848, pages 125–137. International Society for Optics and Photonics, 2002.

J. H. M. M. Schmitt, K.-P. Schröder, G. Rauw, A. Hempelmann, M. Mittag, J. N. González-Pérez, S. Czesla, U. Wolter, D. Jack, P. Eenens, et al. Tigre: A new robotic spectroscopy telescope at guanajuato, mexico. *Astronomische Nachrichten*, 335(8):787–796, 2014.

H. Kaushal, V. K. Jain, and S. Kar. *Free Space Optical Communication*. Springer (India), 2017.

D. A. Bristow, M. Tharayil, and A. G. Alleyne. A survey of iterative learning control. *IEEE Control Systems Magazine*, 26(3):96–114, 2006.

Pre-Print version of the article: Thomas Riel, Andreas Sinn, Christian Schwaer, Martin Ploner, Georg Schitter, "Iterative Trajectory Learning for Highly Accurate Optical Satellite Tracking Systems", *Acta Astronautica*, vol. 164, pp. 121-129, 2019. DOI: 10.1016/j.actaastro.2019.07.012

H. W. Yoo, S. Ito, and G. Schitter. High speed laser scanning microscopy by iterative learning control of a galvanometer scanner. *Control Engineering Practice*, 50:12 – 21, 2016.

K. Riesing, H. Yoon, and K. Cahoy. A portable optical ground station for low-earth orbit satellite communications. In *2017 IEEE International Conference on Space Optical Systems and Applications (ICSOS)*, pages 108–114, 2017.

T. Riel, R. Saathof, A. Katalenic, S. Ito, and G. Schitter. Noise analysis and efficiency improvement of a pulse-width modulated permanent magnet synchronous motor by dynamic error budgeting. *Mechatronics*, 50:225–233, 2017.

T. Riel, A. Galffy, and G. Schitter. Analysis and robust control of an precision motion platform using disturbance compensation. In *Proceedings of the IEEE Conference on Control Technology and Applications (CCTA), Copenhagen, Denmark*, pages 1090–1095, 2018.

R. Berry and J. Burnell. *Astronomical Image Processing*. Willman-Bell Inc, 2000.

D. de Roover. Synthesis of a robust iterative learning controller using an h_∞ approach. In *Decision and Control, 1996., Proceedings of the 35th IEEE Conference on*, volume 3, pages 3044–3049. IEEE, 1996.

D. Lang, D. W. Hogg, K. Mierle, M. Blanton, and S. Roweis. Astrometry. net: Blind astrometric calibration of arbitrary astronomical images. *The astronomical journal*, 139(5):1782, 2010.

M. R. Calabretta and E. W. Greisen. Representations of celestial coordinates in fits. *Astronomy & Astrophysics*, 395(3):1077–1122, 2002.

G. Seeber. *Satellite geodesy: foundations, methods, and applications*. Walter de gruyter, 2008.

M. R. Pearlman, J. J. Degnan, and J. M. Bosworth. The international laser ranging service. *Advances in Space Research*, 30(2):135–143, 2002.

C. E. Noll. Crustal dynamics data information system. slr orbit predictions. ftp://cddis.gsfc.nasa.gov/slr/cpf_predicts/current/, 2018. Accessed: 27.09.2018.

T. S. Kelso. Celestrak. public domain satellite tracking data. www.celestrak.com/NORAD/elements/, 2018. Accessed: 27.09.2018.

C. Rino. Satellite orbit computation - modified sgp4 code for gps interface. de.mathworks.com/matlabcentral/fileexchange/28888-satellite-orbit-computation, 2010. Accessed: 27.02.2019.

Pre-Print version of the article: Thomas Riel, Andreas Sinn, Christian Schwaer, Martin Ploner, Georg Schitter, "Iterative Trajectory Learning for Highly Accurate Optical Satellite Tracking Systems", *Acta Astronautica*, vol. 164, pp. 121-129, 2019. DOI: 10.1016/j.actaastro.2019.07.012

W. Gurtner and R. Ricklefs. Consolidated prediction format sample code suite. ilrs.cddis.eosdis.nasa.gov/docs/2017/cpf_sample_code_v1.01d.tgz, 2005. Accessed: 27.02.2019.

Pre-Print version of the article: Thomas Riel, Andreas Sinn, Christian Schwaer, Martin Ploner, Georg Schitter, "Iterative Trajectory Learning for Highly Accurate Optical Satellite Tracking Systems", *Acta Astronautica*, vol. 164, pp. 121-129, 2019. DOI: 10.1016/j.actaastro.2019.07.012